DNA electrophoretic collisions with single obstacles

Grant I. Nixon and Gary W. Slater*

Department of Physics, University of Ottawa, 150 Louis Pasteur, Ottawa, Ontario, Canada K1N 6N5

(Received 25 May 1994)

We analyze the electrophoretic collision between an obstacle, such as a gel fiber, and a large diffusing polyelectrolyte. This type of collision may be considered as the basic unit of elementary sieving behind all electrophoretic separation methods. The polymer first hooks around an obstacle and must escape using a simple "pulley" process which requires a molecular-size-dependent time. We demonstrate, using both analytical and simulation results, that simple isolated collisions cannot lead to separation due to large diffusion effects generated by the process (in spite of the stacking phenomenon).

INTRODUCTION

Electrophoresis is the commonly used method for separating polyelectrolytes, such as DNA, according to molecular size (as in the human genome project [1]). Since polyelectrolytes in solution behave like free-draining coils, one must use gel electrophoresis for separation. There, the gel is believed to act like a molecular sieve, discriminating on the basis of molecular size [2]. Recently, regular arrays of microlithographically constructed cylindrical posts [3], entangled [4] and unentangled [5] polymer solutions, as well as various porous systems [6] have been used as electrophoretic sieving media.

Theoretical studies of gel electrophoresis have usually been based on the reptation concept [7–9], on the so-called Ogston sieving model [10], and on simulations [11,12]. Of foremost importance is the effect of DNA-gel fiber collisions on the mobility, diffusion, and conformation of the DNA. A complete understanding of gel electrophoresis requires a theory which can explain the interrelation among these elements. When DNA collides simultaneously with many gel fibers, such an understanding is almost inextricable. The reptation concept uses a mean-field-like approach to these DNA-fiber interactions. This is clearly an oversimplification, although it permits an analytical treatment [13]. Obukhov and Rubinstein [14] have, however, demonstrated that multiple interactions may indeed change the qualitative nature of the drift.

Our aim is to (i) conduct a diagnostic of a collision between a DNA chain and an isolated obstacle, (ii) develop a simple quantitative model of the collision, and (iii) determine if such isolated events yield effective separation. We do not consider DNA-obstacle frictional interactions [15]; however, unlike a similar study [16], we treat both electrophoretic mobility *and* diffusion, since the resolution of electrophoretic molecular bands is affected by both of these transport properties.

SIMULATION METHOD

The electrophoretic collision between a Rouse-like bead-spring free-draining polyelectrolyte and a circular obstacle was simulated using a two-dimensional (2D) Brownian dynamics algorithm. The molecule is first guided down a narrow channel (such as a pathway within a gel matrix) towards a circular obstacle (or gel fiber) under the influence of an applied electric field E. Figure 1 contains snapshots of a molecule as it migrates down the channel. Our depiction of the collision process is much like those of recent experiments [3,17,18]. The chain is composed of M beads, each of charge q and friction coefficient ξ, connected via $M-1$ massless anharmonic springs whose maximal extension L serves as a unit length. In 2D, the entropic force $F_{spring}(\Delta r)$ between the two ends of a spring of extension Δr is given through inversion of the equation $\Delta r(f_a) = \partial \ln[I_0(f_a)]/\partial f_a$, where I_v is the modified Bessel function of order v, $f_a = F_{spring}a/(k_B T)$ is the scaled spring force, and $a = L/N$ is the Kuhn length of the N freely jointed polymer segments comprising each spring [19]. The channel walls and the circular obstacle (both hard cores) have soft-core potentials extending beyond their boundaries over a distance $\sigma/L = 0.02$–0.05. The equation of motion for each bead is solved numerically using a small but *self-adjusting* time increment $\Delta\tau$ following a technique we developed [20]. In the absence of collisions, chains follow the typical Rouse dynamics of free-draining coils. Excluded volume, hydrodynamics, and Coulombic repulsion between beads are not considered. The time unit is $\tau_L = \xi L^2/(2k_B T)$ and the dimensionless electric field intensity is $\varepsilon = qEL/(2k_B T)$. The obstacle radius $R_{obs} = L/2$ was chosen so as to keep the springs from moving through the obstacle.

*Author to whom correspondence should be addressed.
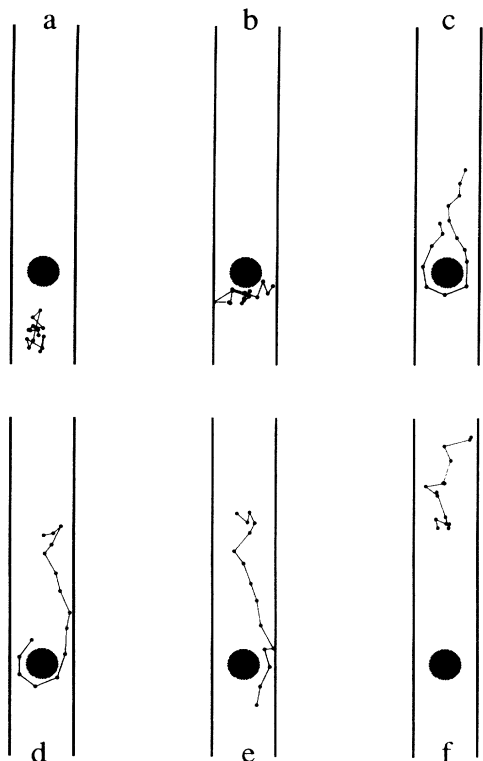Electronic address: gary@physics.uottawa.ca

FIG. 1. Simulation snapshots of the collision between a charged bead-spring polymer and a circular obstacle. The obstacle diameter and the maximum spring extension are both equal to 1, the tube width is 2, its length is 11, the scaled field is $\varepsilon = 1$, and the molecular size is $M = 15$ beads. (a) $t = 62/12$: the random-walk chain drifts towards the obstacle. (b) $t = 97/12$: the molecule collides with the obstacle and starts deforming. This leads to stacking. (c) $t = 167/12$: the molecule adopts a U-shaped conformation about the obstacle which acts like a pulley. (d) $t = 219/12$: the tug-of-war between the two arms results in cannibalization of the short one. (e) $t = 245/12$: the chain is now free but strongly oriented. The distance between the center of mass of the chain and the obstacle's center is approximately half the end-to-end distance. (f) $t = 284/12$: the chain now slowly relaxes back to a random-walk conformation while swiftly drifting away from the obstacle.

SIMULATION RESULTS

We analyzed numerous chain properties in order to yield a complete diagnostic of the collision. Figures 2–4 indicate how the mean (longitudinal) position of the center of mass (c.m.), $\langle y(t) \rangle$, its variance $\langle \Delta y^2(t) \rangle = \langle y^2(t) \rangle - \langle y(t) \rangle^2$, the mean square end-to-end distances of the chain, $\langle h_y^2(t) \rangle$ and $\langle h_x^2(t) \rangle$, and the variance of the motion in the transverse direction, $\langle \Delta x^2(t) \rangle = \langle x^2(t) \rangle - \langle x(t) \rangle^2$, vary with time. These averages were generated over an ensemble of 867 molecules, each starting (with differing initial conformations) from a distance of $15L$ from the center of the obstacle. Since the field intensity was $\varepsilon = 1.0$, the free-drift velocity is $V_0 = \varepsilon = 1.0$ in our scaled units, irrespective of the molecular size M. It is indeed because of this free-
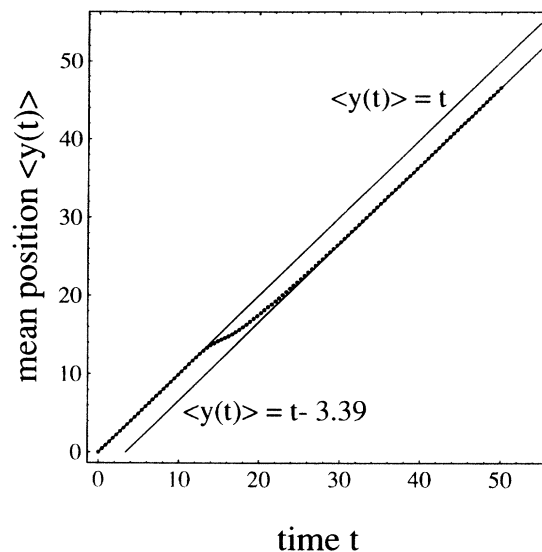

FIG. 2. The mean position of the center of mass along the tube axis, $\langle y(t) \rangle$, vs time t for a population of 867 molecules. The conditions are as described in Fig. 1. The molecules begin at position $y(0) = 0$ with the obstacle centered at position $y = 15$. The collision retards the molecule, which is equivalent to a free-drift of duration (or distance) 3.39, as shown.

draining behavior that one must use the sieving properties of a separation medium in order to separate DNA molecules according to molecular size [1,2]. Figure 2 shows that the collision [Figs. 1(b)–1(d)] leads to a loss of about $\tau_{retardation} = 3.4$ time units. Figure 3 indicates that $\langle h_x^2(t) \rangle$ increases during the collision; this is due to the chain forming a pulley [Figs. 1(c)–1(d)] around the obsta-
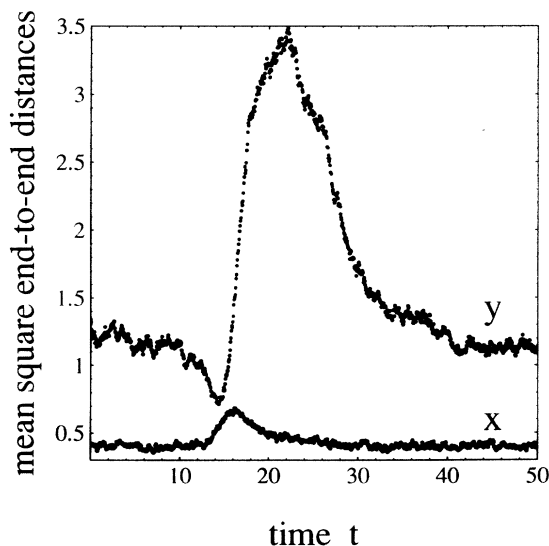

FIG. 3. Mean square end-to-end distance vs time t. In the (y) direction parallel to the tube axis, the end-to-end distance and the radius of gyration (not shown) undergo a small decrease (the stacking effect) followed by a large increase. In the (x) transverse direction, a large increase is also observed but lasts for a shorter period of time (about 10 time units).
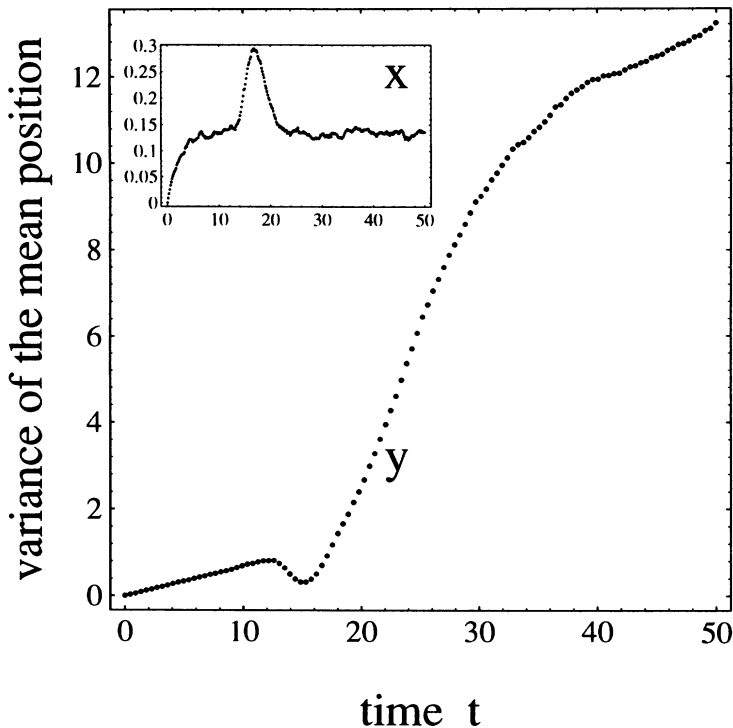
FIG. 4. Variance of the position of the center of mass vs time t. In the (x) transverse direction, the variance first saturates (because of confinement), and then rises through a maximum with a time width of about 10 units. In the (y) parallel direction, the variance first decreases (again the stacking effect), but then increases more than an order of magnitude before finally recovering normal behavior after the collision.

cle with $\max[\langle h_x^2(t)\rangle^{1/2}]\approx 0.83\approx 2R_{obst}=1.0$. We also note that the onset of collision occurs at $t\approx 13$ and terminates at $t\approx 25$. In the parallel direction, the end-to-end distance goes through a "stacking" phase between $t\approx 13$ and $t\approx 15$ where the chain is compressed, a stretching phase between $t\approx 15$ and $t\approx 22$ where $\langle h_y^2(t)\rangle$ more than doubles, and finally a relaxation phase extending to a time $t\approx 45$. The Rouse time for this chain is $\tau_{Rouse}\approx 3.5$ in the parallel direction; therefore, the long relaxation tail is due mostly to chains requiring more time to escape from the obstacle [Figs. 1(c)–1(e)]. The molecular orientations displayed in Figs. 1(c)–1(e) and Fig. 3 have been observed experimentally [3,17,18,21]. Figure 4 displays the variance for the position of the c.m. in both directions. In the transverse (x) direction, it first increases very quickly and saturates at time $t\approx 8$ because the chain is confined within a narrow tube; it then goes through a large maximum [with $\sqrt{\langle\Delta x^2(t)\rangle}\approx 0.54\approx R_{obst}$, as expected] during the collision. The variance of $y(t)$ displays normal free-drift (Rouse) diffusion behavior before [Fig. 1(a)] and after [Fig. 1(f)] the collision. There is also a stacking effect at time $t\approx 15$: the small dip is due to the faster-moving chains hitting the obstacle first, thus allowing slower-moving chains time to catch up [see Fig. 1(b)]. However, Fig. 4 indicates a catastrophic increase of the spatial dispersion following the stacking phase. Normal diffusion behavior is recovered for times $t>45$, which coincides with the time where normal end-to-end distances h_y are recovered (Fig. 3). The large increase of the spatial dispersion is due to the first molecules escaping and free-drifting far ahead of the last molecules to escape. The dispersion of escape times thus leads to a large increase in band broadening (spatial dispersion).

A SIMPLE MODEL

Two factors are of foremost importance for any electrophoretic system used to separate polydisperse molecules: the molecular-size dependent retardation due to the sieving properties of the collisions between the migrating molecules and the separation matrix, and the net dispersion (diffusion) of the molecules due to these collisions. One seeks to maximize the former and to minimize the latter. In this section, we present a simple semiquantitative model of an isolated collision in the large field and large molecular size limit.

The simplest nontrivial polyelectrolyte-matrix interaction is shown schematically in Fig. 1. The chain forms a pulley where each arm first attains maximum extension before unravelling begins. Initially let the arms have n_1 and n_2 springs, with $n_1+n_2=M-1\approx M\gg 1$. The essential features describing the dynamics of such processes are but slightly affected by the choice of distribution function for the initial value of the impact parameter $m=|n_1-n_2|$, as we will demonstrate.

If we assume that the coil's center-of-mass is centered over the obstacle, then the way in which the polymer coil unravels and adopts a pulleylike conformation (just after the onset of collision) may be viewed as a random process. The initial distribution function of m is then given by the Gaussian function

$$p_G(m)=[2/(\pi M)]^{1/2}e^{-m^2/2M}.\qquad(1)$$

Alternatively, if the collision itself is seen as the random event, occurring with equal likelihood anywhere along the chain, then the appropriate distribution function for m would be uniform over the interval 0 to M:

$$p_U(m) = 1/M \; . \tag{2}$$

If all events result in a collision, then these two distributions represent two extreme limits with $\langle m \rangle_G \sim M^{1/2}$ and $\langle m \rangle_u \sim M$.

We may estimate the mean-spring extension λ_z, for a branch comprised of one fixed end and z springs, using the force law for the springs $\Delta r(f)$:

$$\lambda_z = \overline{\Delta r_z} \approx \frac{1}{z} \int_0^z dj \, \Delta r \left[j \frac{qEa}{k_B T} \right] = \frac{N}{2z\varepsilon} \ln[I_0(2z\varepsilon/N)]$$

$$\approx 1 - \frac{\ln(4\pi z\varepsilon/N)}{4z\varepsilon/N} \; . \tag{3}$$

As we can see, in the large field and large molecular size limit, the second term is merely a correction factor that vanishes for $z \to \infty$ or $\varepsilon \to \infty$. For simplicity, we assume that the mean spring extension during the whole collision process is given by $\lambda_{z \to M/2}$:

$$\lambda \approx 1 - \frac{\ln(2\pi M\varepsilon/N)}{2M\varepsilon/N} \; . \tag{4}$$

With $M=15$, $N=5$, and $\varepsilon=1$, as in our simulations, we yield $\lambda \approx 0.51$, in qualitative agreement with Fig. 1, which shows that during the collision [Figs. 1(c)–1(e)] the springs reach approximately 50% of their maximum extension (the diameter of the obstacle is 1.0).

When the pulley is formed [Fig. 1(c)], the spring stress is maximal and the long arm cannibalizes the short one. The pulley formation time is approximately the time required for the last bead of either arm to free-drift, with velocity $V_0 = \varepsilon$, to its final position within the pulley. Thus, the time to reach full extension may be taken as approximately $\tau_{\text{pulley}} \approx M\lambda/(2\varepsilon)$, where $M\lambda/2$ is the mean arm length and λ is the mean spring extension. In view of Eq. (4), we may thus express the mean pulley time as

$$\tau_{\text{pulley}} \approx \frac{M\lambda}{2\varepsilon} \approx \frac{M}{2\varepsilon} \left[1 - \frac{\ln(2\pi M\varepsilon/N)}{2M\varepsilon/N} \right] \; . \tag{5}$$

With $M=15$, $N=5$, and $\varepsilon=1$, as used in our simulations, we yield $\lambda \approx 0.51$ (as noted before) with a corresponding escape time $\tau_{\text{pulley}} \approx 3.8$. This pulley formation time is in good agreement with the time required for $\langle h_x^2 \rangle$ to attain its maximum value (see Fig. 3).

The escape time from the pulley conformation is found simply by solving the equation of motion for an inextensible rope (assuming that the springs keep their mean extension λ during the process) on a pulley in the presence of a force qE on each element (bead) [16,20,22]:

$$\tau_{\text{escape}}(m) = \ln \left[\frac{M}{m} \right] \tau_{\text{pulley}} \; . \tag{6}$$

We note that this time diverges for $m=0$. A solution including the effects of Brownian motion does not show this divergence [16]. However, Brownian motion complicates matters unnecessarily, as this divergence carries little weight when averaged over the distribution functions for m. Indeed, using Eq. (1), we find that

$$\langle \tau_{\text{escape}} \rangle_G = \tfrac{1}{2} [\gamma + \ln(2M)] \tau_{\text{pulley}} \; , \tag{7}$$

where $\gamma \approx 0.5772\ldots$ is Euler's constant, while, using Eq. (2), we have

$$\langle \tau_{\text{escape}} \rangle_U = \tau_{\text{pulley}} \; . \tag{8}$$

The two results differ only by a logarithmic factor ($\sim \ln M$). Thus the corresponding values are (for $\varepsilon=1$, $N=5$, and $M=15$) $\langle \tau_{\text{escape}} \rangle_G \approx 7.6$ and $\langle \tau_{\text{escape}} \rangle_U \approx 4.0$. Using Eqs. (1)–(5), we yield the mean net collision times

$$\langle \tau_{\text{coll}} \rangle_G \approx \tau_{\text{pulley}} + \langle \tau_{\text{escape}} \rangle_G$$

$$\approx \tfrac{1}{2} [2 + \gamma + \ln(2M)] \tau_{\text{pulley}} \tag{9}$$

and

$$\langle \tau_{\text{coll}} \rangle_U \approx 2\tau_{\text{pulley}} \; . \tag{10}$$

For our simulations (using $\varepsilon=1$ and $N=5$) for $M=15$ bead chains, we have $\langle \tau_{\text{coll}} \rangle_G \approx 11.4$ and $\langle \tau_{\text{coll}} \rangle_U \approx 7.6$ both values agreeing qualitatively with Figs. 3 and 4, with a mean collision time (measured using data for the x direction, for which Rouse relaxation does not play a role) of about $\langle \tau_{\text{coll}} \rangle \approx 10$.

The retardation time due to collision is τ_{coll} minus the time τ_0 required to free-drift over the same distance [which is approximately $M\lambda/2$; see Fig. 1(e)] in absence of the obstacle

$$\tau_0 \approx \frac{M\lambda}{2\varepsilon} = \tau_{\text{pulley}} \; . \tag{11}$$

Thus $\langle \tau_{\text{retardation}} \rangle_G \approx \langle \tau_{\text{escape}} \rangle_G = 7.6$ and $\langle \tau_{\text{retardation}} \rangle_U \approx \langle \tau_{\text{escape}} \rangle_U = 3.8$, while the simulations yield $\tau_{\text{retardation}} \approx 3.4$ (see Fig. 2). The uniform ensemble yields the best results in part because some of the $M=15$ bead chains do not form complete pulley conformations and quickly slide off the obstacle to the side. In such cases, giving conformations with large values of m equal weight inevitably reduces the overall value of the mean escape time. The retardation time increases almost linearly with size M for large M (simulations with $M=10$–40 agree with this scaling [20]).

From Eqs. (1)–(6) we yield the escape time variances

$$\langle \Delta \tau_{\text{escape}}^2 \rangle_G = \langle \tau_{\text{escape}}^2 \rangle_G - \langle \tau_{\text{escape}} \rangle_G^2$$

$$= \frac{\pi^2}{8} \tau_{\text{pulley}}^2 \; , \tag{12}$$

and

$$\langle \Delta \tau_{\text{escape}}^2 \rangle_U = \tau_{\text{pulley}}^2 \; . \tag{13}$$

Hence the variance of escape times is little affected by the nature of the collision process, both scaling roughly as M^2 and differing functionally only by a numerical coefficient $\pi^2/8$. The molecules therefore unhook over a wide range of escape times, the escape time being a function of the initial value of m at the time of formation of the pulley. These temporal variances lead to corresponding spatial variances of the molecules:

$$\langle \Delta y_{\text{escape}}^2 \rangle \approx \frac{V_0^2}{2} \Delta \tau_{\text{escape}}^2 \approx \frac{\varepsilon^2}{2} \tau_{\text{pulley}}^2 \approx \frac{M^2 \lambda^2}{8} \; . \tag{14}$$

Under our simulation conditions, this yields $\langle \Delta y^2_{escape} \rangle \approx 10$, in good agreement with our simulation results, which show an increase of about 9 during the collision (Fig. 4). Of course, this spatial dispersion is much larger than what would be expected from normal Rouse dynamics (i.e., from what is observed in the absence of such collisions). Hence the variance of escape times is *the* major cause of spatial dispersion (the Rouse diffusion coefficient decreases as $1/M$). Remarkably, we find that the spatial variance is, in fact, a weak function of electric field (via λ) but is a strongly increasing function of molecular size.

DISCUSSION

We have presented data for the high-field collision of a $M = 15$ bead Rouse chain with a large obstacle in a narrow channel. The diagnostic of the collision indicates that the escape process is not specific enough to lead to efficient electrophoretic separation: the large range of escape times leads to a catastrophic increase of molecular diffusion (band broadening). Even though the distance lost during the collision $\langle y_{retardation} \rangle = V_0 \langle \tau_{retardation} \rangle \approx V_0 \langle \tau_{escape} \rangle$ is a strong function of the molecular size M [i.e., $\langle y_{retardation} \rangle_G \sim M \ln M$ for the Gaussian distribution Eq. (1) and $\langle y_{retardation} \rangle_U \sim M$ for the uniform distribution Eq. (2)], the fact that its standard deviation $\Delta y_{retardation} \approx \langle \Delta y^2_{escape} \rangle^{1/2} \sim M$ also increases with M makes it impossible to use such single isolated collisions as a means of separation. Moreover, the resolution factor [23] $(\partial y_{retardation}/\partial M)/(\Delta y_{retardation})$ vanishes for large M; i.e.,

$$\frac{\left| \dfrac{\partial \langle y_{retardation} \rangle_G}{\partial M} \right|}{(\langle \Delta y_{retardation} \rangle_G)} \sim \frac{\ln M}{M}$$

and

$$\frac{\left| \dfrac{\partial \langle y_{retardation} \rangle_U}{\partial M} \right|}{(\langle \Delta y_{retardation} \rangle_U)} \sim \frac{1}{M}.$$

It is therefore the nonspecificity of the collision process that renders it useless for separation. However, multiple, simultaneous collisions, like those occurring in gels, lead to different physics. For low fields, the reptation concept may be adapted to account for fluctuations of the chain [9]. In the high field limit, chains take on self-similar conformations [14] and multiple loops compete for growth. Diffusion is not well understood under such conditions; unfortunately, it is indeed diffusion that limits the efficiency of electrophoresis-based sequencing systems [23].

We have also discussed the problem from the dual viewpoints of the Gaussian and the uniform distributions. Both have their strengths: the Gaussian distribution is more representative in the cases where the tube acts as a lens and keeps the center-of-mass relatively centered (focused) over the obstacle before the collision; the unraveling may then be taken as a random process. On the other hand, if the tube is not too narrow, the position of the obstacle, upon impact, along the polyelectrolytic coil may be taken as a random process; some coils in fact do not form U shapes in our system and, therefore, they escape quite rapidly. Evidently, in the situation studied here, there is a melding of the two viewpoints and our results seem to corroborate this fact. Our main goal has been merely to speculate on the dynamics with, admittedly, simplified models and to deduce the proper scaling forms. Interestingly, the choice of distribution is of little consequence with regard to the scaling forms.

In the near future, we will investigate situations where the polymer chains become entropically trapped for low fields in inhomogeneous environments [24]. Here, one requires a minimum field intensity to deform the molecule and force it through the narrow openings [20,25]. In the limit where the radius of gyration is comparable to the pore or channel size, and for low field intensity, the dynamics is governed by entropic and sieving effects which cannot be described by the model presented here. Although these effects have been reported [20,24,25], they may not be important under normal sequencing conditions.

ACKNOWLEDGMENTS

[1] G. W. Slater, P. Mayer, and G. Drouin, Analusis **21**, M25 (1993).

[2] B. H. Zimm and S. D. Levene, Rev. Biophys. **25**, 171 (1992).

[3] W. D. Volkmuth and R. H. Austin, Nature **358**, 600 (1992).

[4] P. D. Grossman and D. S. Soane, J. Chromatogr. **559**, 257 (1991).

[5] A. E. Barron, D. S. Soane, and H. W. Blanch, J. Chromatogr. A **652**, 3 (1993).

[6] M. G. Harrington, K. H. Lee, J. E. Bailey, and L. E. Hood, Electrophoresis **15**, 187 (1994).

[7] O. J. Lumpkin, P. Déjardin, and B. H. Zimm, Biopolymers **24**, 1573 (1985).

[8] J. Noolandi, J. Rousseau, and G. W. Slater, Phys. Rev. Lett. **58**, 2428 (1987).

[9] T. A. J. Duke, A. N. Semenov, and J. L. Viovy, Phys. Rev. Lett. **69**, 3260 (1992).

[10] D. Rodbard and A. Chrambach, Proc. Natl. Acad. Sci. USA **4**, 970 (1970).

[11] J. M. Deutsch, Science **240**, 922 (1988).

[12] T. A. J. Duke and J. L. Viovy, Phys. Rev. Lett. **68**, 542

(1992).

[13] G. W. Slater, Electrophoresis **14**, 1 (1993).

[14] S. P. Obukhov and M. Rubinstein, J. Phys. II (France) **3**, 1455 (1993).

[15] S. Burlatsky and J. Deutch, Science **260**, 1782 (1993).

[16] W. D. Volkmuth, T. Duke, M. C. Wu, R. H. Austin, and A. Szabo, Phys. Rev. Lett. **72**, 2117 (1994).

[17] D. C. Schwartz and M. Koval, Nature (London) **338**, 520 (1987).

[18] S. Gurrieri, E. Rizzarelli, D. Beach, and C. Bustamante, Biochemistry **29**, 3396 (1990).

[19] G. W. Slater, S. J. Hubert, and G. I. Nixon, Macromol.

Theory Simul. **3**, 695 (1994).

[20] G. I. Nixon, M. Sc. Thesis, University of Ottawa (1994).

[21] S. B. Smith, P. K. Aldridge, and J. B. Callis, Science **243**, 203 (1989).

[22] H. A. Lim, G. W. Slater, and J. Noolandi, J. Chem. Phys. **92**, 709 (1990).

[23] J. A. Luckey, and L. M. Smith, Anal. Chem. **65**, 2841 (1993).

[24] D. A. Hoagland and M. Muthukumar, Macromolecules **25**, 6696 (1992).

[25] P. Mayer, G. W. Slater, and G. Drouin, Appl. Theor. Electrophor. **3**, 147 (1993).
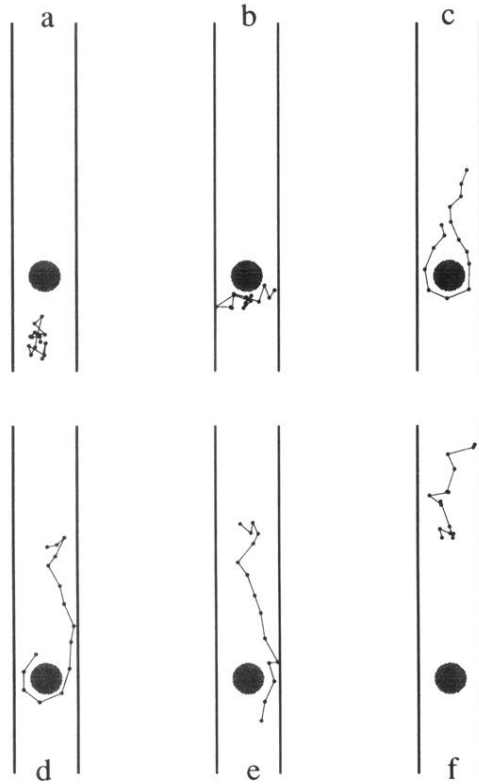
FIG. 1. Simulation snapshots of the collision between a charged bead-spring polymer and a circular obstacle. The obstacle diameter and the maximum spring extension are both equal to 1, the tube width is 2, its length is 11, the scaled field is $\varepsilon = 1$, and the molecular size is $M = 15$ beads. (a) $t = 62/12$: the random-walk chain drifts towards the obstacle. (b) $t = 97/12$: the molecule collides with the obstacle and starts deforming. This leads to stacking. (c) $t = 167/12$: the molecule adopts a U-shaped conformation about the obstacle which acts like a pulley. (d) $t = 219/12$: the tug-of-war between the two arms results in cannibalization of the short one. (e) $t = 245/12$: the chain is now free but strongly oriented. The distance between the center of mass of the chain and the obstacle's center is approximately half the end-to-end distance. (f) $t = 284/12$: the chain now slowly relaxes back to a random-walk conformation while swiftly drifting away from the obstacle.